Supporting Information

Highly Stretchable Ionotronic Pressure Sensors with Broad Response Range Enabled by Microstructured Ionogel Electrodes

*Zhenkai Huang, Yutong Chen, Jianping Peng, Tianrui Huang, Faqi Hu, Xiang Liu, Liguo Xu, Kan Yue**

Dr. Z. Huang, Y. Chen, T. Huang, F. Hu, X. Liu, Prof. K. Yue
South China Advanced Institute for Soft Matter Science and Technology
School of Emergent Soft Matter
South China University of Technology
Guangzhou 510640, China
E-mail: kanyue@scut.edu.cn

Dr. Z. Huang
School of Materials Science and Hydrogen Energy
Foshan University
Foshan 528000, China

Dr. J. Peng
School of Environmental and Chemical Engineering
Foshan University
Foshan 528000, China

Dr. L. Xu
College of Light Chemical Industry and Materials Engineering
Shunde Polytechnic
Foshan 528333, China

Prof. K. Yue
Guangdong Provincial Key Laboratory of Functional and Intelligent Hybrid Materials and Devices
South China University of Technology
Guangzhou 510640, China

Dr. Z. Huang and Y. Chen contributed equally to this work.

This material includes

Experimental Section

1. Chemicals and Solvents

2,2,2-Trifluoroethyl acrylate (TFEA, 98%) was purchased from Shanghai Qinba Chemical Co., Ltd., China. 1-Ethyl-3-methylimidazolium bis(trifluoromethylsulfonyl)imide ([EMIM][TFSI], 98%) was obtained from Monils Chemical (Shanghai) Co., Ltd., China. 2-Hydroxy-4'-(2-hydroxyethoxy)-2-methylpropiophenone (Irgacure 2959, 99%), acrylamide (AAm, 99%), ethylene dimethacrylate (EGDMA, 98%), and all solvents were purchased from Shanghai Titan Scientific Co., Ltd. All chemicals were used as received without further purification.

2. Preparation of Ionogels as the Ionotronic Electrodes

The schematic illustrations for the chemical structure and preparation procedure of the ionogel as the ionotronic electrodes were shown in Fig. 2a and b. First, an ionogel system adapted from our previously reported P(TFEA-*co*-AAm)-[EMIM][TFSI] ionogel was used as the ionotronic electrodes. In a typical procedure, AAm (1.2 g), TFEA (5.2 g) and EGDMA (201 mg) were mixed with [EMIM][TFSI] (9.6 g) followed by a strong stirring at 45 °C to obtain a well dispersed solution. After the addition of Irgacure 2959 (11 mg), the mixture was allowed to polymerize for 2 h under the irradiation of UV light (365 nm) to obtain the final ionogel, in which the molar ratio of AAm to TFEA was 50%, the polymer mass fraction was 40%, and the cross-linker molar content was 2%. The ionogel in this composition was denoted as Ionogel-4050-2%. To systematically study the properties of ionogels with different compositions, a series of ionogels with different cross-linker molar contents were prepared following the same procedure, such as Ionogel-4050-0.5%, Ionogel-4050-1%, Ionogel-4050-2% and Ionogel-4050-5%.

To realize the proposed human skin-inspired microstructures on the surface of ionotronic electrodes, we adopted commercial sandpapers (3M Corporation) with different roughness (mesh size) as the templates. The unpolymerized solution was poured onto the custom-made molds with sandpaper templates in one side and cured under the irradiation of UV light (365 nm) for 2 h, followed by demolding. Finally, the ionotronic electrodes with and without microstructures were cut into different sizes such as 10 mm × 10 mm × 1 mm and 20 mm × 6 mm × 1 mm for different types of configurations.

3. Fabrication of the iCPS

The schematic illustration of the bio-inspired stretchable ionotronic capacitive pressure sensor (iCPS) was shown in Fig. 3a. The PDMS dielectric thin film (thickness: 100 μm, Dow Corning Co., Ltd.) was sandwiched between two microstructured ionotronic electrodes. Copper sheets adhered on the ionotronic electrodes were used as current collectors. Finally, the stretchable pressure sensors were encapsulated with two PDMS thin films with the help of 3M VHB tapes. The photograph showing the structure of our assembled iCPS was shown in Fig. S20, Supporting Information.

4. Finite Element Analysis

FEA was performed using the commercial package ABAQUS 6.14. Two-dimensional model was built for simplicity. The structure of electrodes and dielectric layer have the same dimensions as in the real sensor. A surface-to-surface frictionless contact between the electrodes and the dielectric layer without penetration was defined. The microstructured ionotronic electrodes and PDMS dielectric thin film were modeled with incompressible Ogden materials and the parameters were obtained by fitting the equiaxial strain-stress data of real materials (Fig. S10). The total contact area was recorded as the pressure increases up to 1 MPa except otherwise noted. The initial contact area A_0 was determined at the pressure of 1 kPa. Detailed stress distribution under various pressures is shown in Fig. 1d. The complete simulation process is provided in the Supplementary Movie.

5. Mechanical Properties

Mechanical testing was performed utilizing an Instron 5965 instrument. Unless otherwise noted, tensile tests were performed at a constant strain rate of 100 mm min^{-1} with a 100 N load cell. Aiming to avoid systematic failure in the vicinity of the clamps, the specimens were cut into dumbbell-shaped samples, with a gauge length of 10 mm, a width of 2 mm, and a thickness of 1.7 mm. For the measurements of resilience, stretching-releasing tests were performed at the same constant strain rate of 100 mm min^{-1} for both stretching and relaxing with various predetermined strains. The compression experiments were performed at a constant compression rate of 1 mm min^{-1} with a 1000 N load cell. The cyclic tensile and compressive tests were performed without rests. The cylindrical specimens were prepared with a diameter of 8 mm and a height of 1.7 mm. Each mechanical test was repeated with at least three individual samples. Finally, the elastic Young's modulus was further calculated from the average slope of strain-stress curves (strain = 10-30%).

6. Fabrication of the Multipixel Sensor Array.

First, the ionotronic electrodes with microstructures were cut to the desired size with a thickness of 1 mm, and then connected with metal wires by adhering copper foils. Next, the ionotronic electrodes were arranged into an array, and a PDMS thin film was placed on top of the ionotronic electrode array as a dielectric layer. Then, another identical ionotronic electrodes array was placed orthogonally to the PDMS dielectric thin film, face-to-face. Finally, the multipixel sensor array was encapsulated with 3M PI tapes to avoid unnecessary charge transfer.

7. Sensing Performances of the iCPS

The dimensions of the iCPS for detailed sensing performances were 10 mm × 10 mm, and the dimensions of the iCPS for sensing performances under unstretched and stretched states were 20 mm × 6 mm, respectively (Fig. S20). All output capacitances were measured on an LCR meter (TH2830, TONGHUI) controlled by a customized LabView program at an AC voltage of 1 V and a sweeping frequency of 1 kHz, unless otherwise specified. The external stretch and/or pressure was applied and measured accurately by using an Instron 5965 instrument. The stability tests were carried out using an electronic universal testing machine (LD22, LISHI Instrument). The measurement of the radial artery pulse wave was carried out by attaching the iCPS to the wrist where the pulse could be detected. The hardness identification of different objects was realized by compressing the target object with a displacement of 0.5 mm and comparing the variations in the capacitance signal. The output signals of the multipixel sensor array were measured with the same LCR meter systems controlled by the customized LabView program at an AC voltage of 1 V and a sweeping frequency of 1 kHz.

8. Other Characterizations

The ionic conductivity of the ionogels in different compositions was determined from the complex impedance plots measured by an electrochemical station (CHI660e, CH Instruments, USA) at room temperatures, over the frequency range from 0.1 Hz to 1 MHz with an amplitude of 10 mV. The bulk resistance (R_b) of the materials was fitted from the Nyquist plot using the Z-view software from the intercept on the real-axis at a high frequency. The ionic conductivity (σ) was then calculated using the relation $\sigma = L/(R_b \times A)$, where ($L$) and ($A$) represent the gauge length and cross-sectional area of the ionic conductor, respectively. The samples were 10 mm × 10 mm with a thickness of 1.7 mm. Attenuated total reflectance Fourier Transform infrared spectroscopy (ATR-FTIR) was carried out on a Nicolet 6700 spectrometer with a diamond ATR crystal as the window material. Scanning electron microscopy (SEM) images were taken on a JSM-7900F microscopy (JEOL).

Fig. S1-S27.

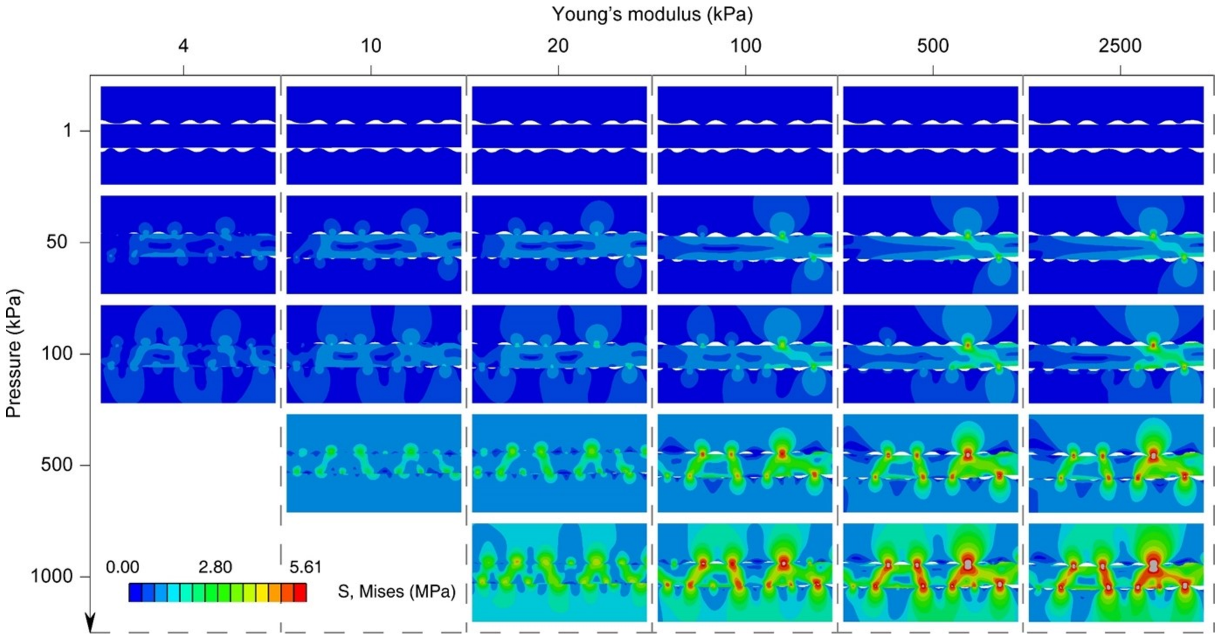

Fig. S1. Compressibility and stress distribution of FEA simulation results with gradient varying given Young's modulus (4 kPa to 2500 kPa) under pressures up to 1 MPa. The FEA simulation was terminated prematurely when the deformation of the microstructured ionotronic electrodes under pressure exceeded the default threshold of the simulation program. The results of early termination are missing from the figure.

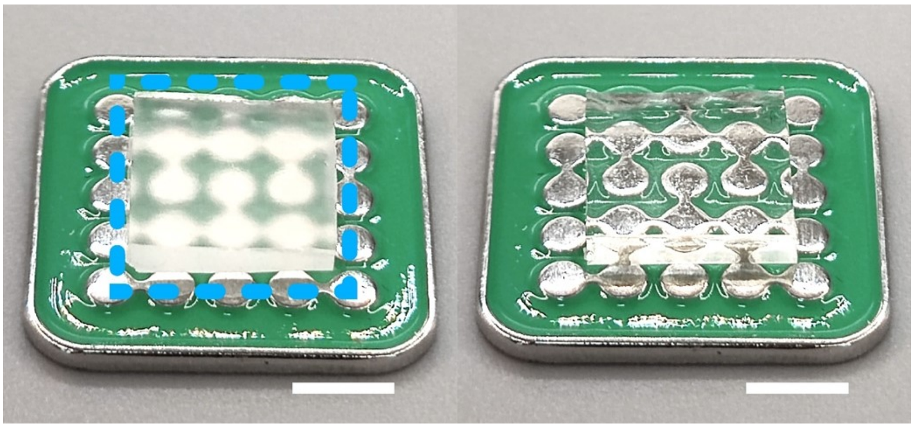

Fig. S2. Optical microscopy images of the ionotronic electrodes with and without microstructures, showing the successful construction of the rough surface from the sandpaper template (scale bar: 5 mm).

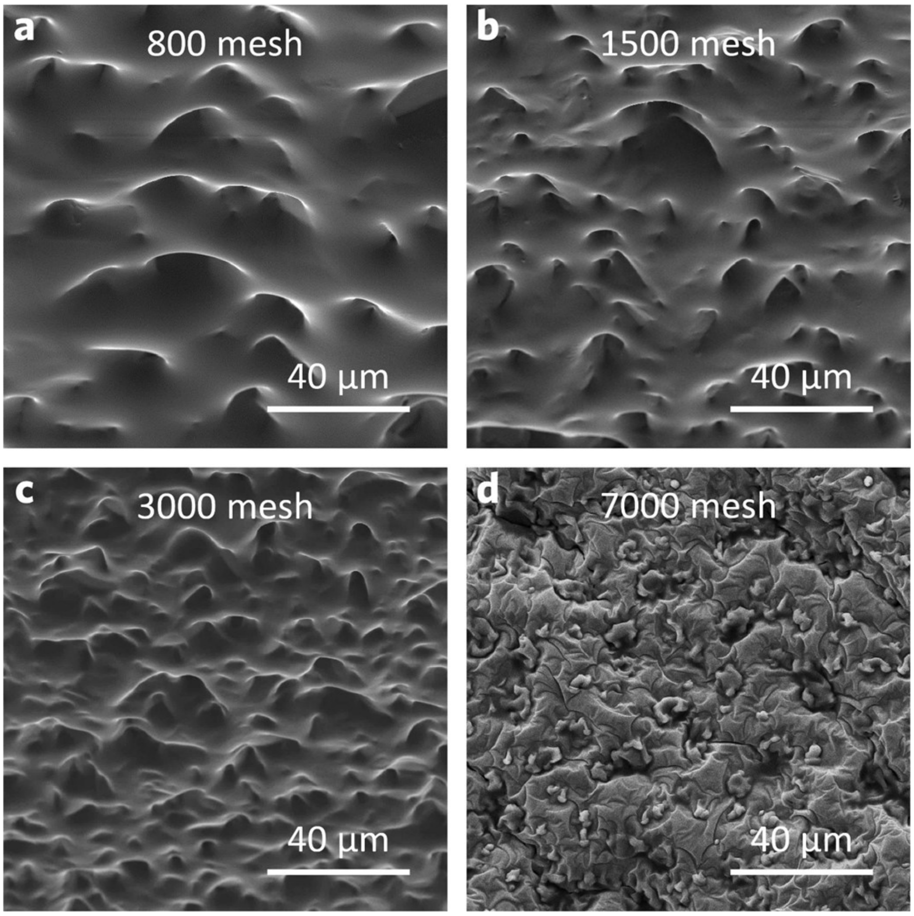

Fig. S3. SEM images of the ionotronic electrodes prepared with 800 **(a)**, 1500 **(b)**, 3000 **(c)** and 7000 **(d)** mesh sandpaper templates, respectively.

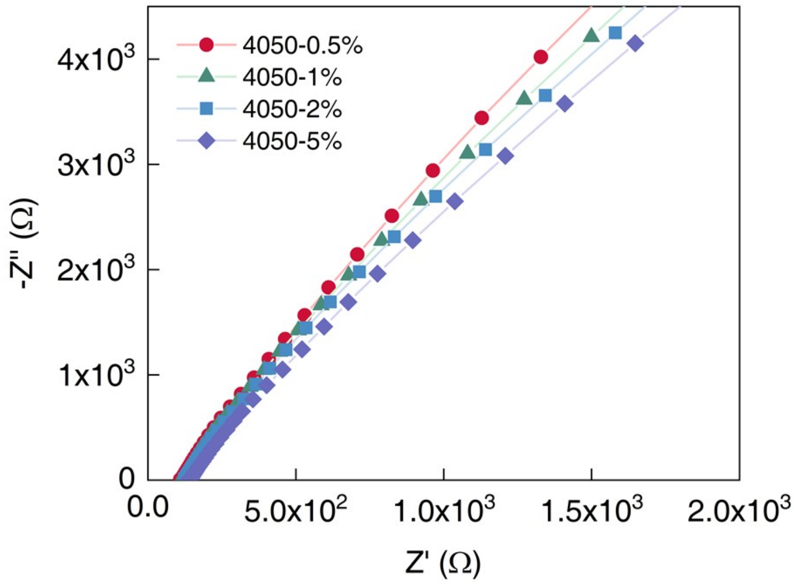

Fig. S4. Nyquist plots of impedance spectra of the ionogels with various EGDMA cross-linker molar content.

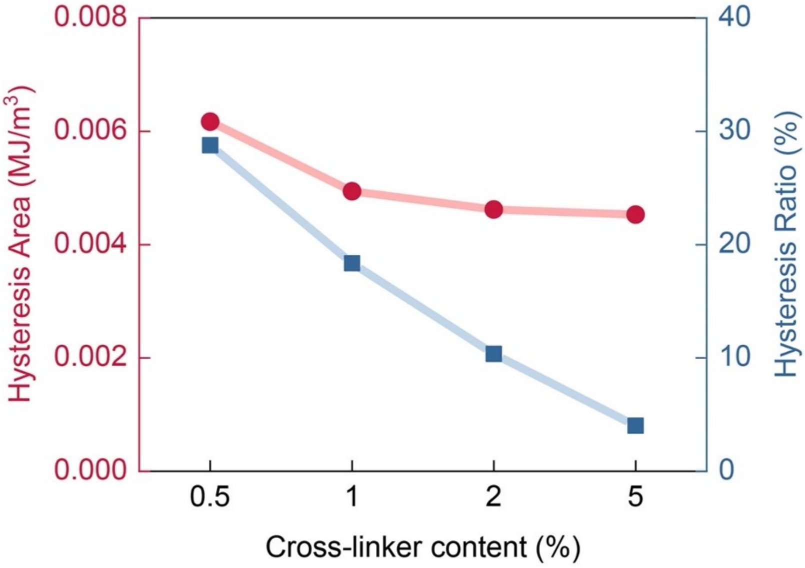

Fig. S5. Plot of hysteresis area and hysteresis ratio versus cross-linker content of the ionogel ranging from 0.5% to 5% at the strain of 100% and the deformation rate of 100 mm min^{-1}.

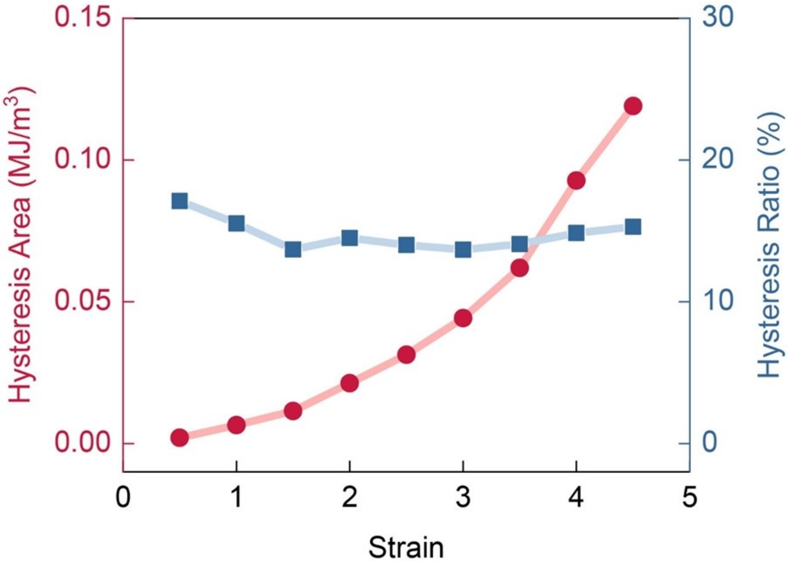

Fig. S6. Plot of hysteresis area and hysteresis ratio versus strain of Ionogel-4050-2% in the strain range from 50% to 450% and break at the deformation rate of 100 mm min^{-1}.

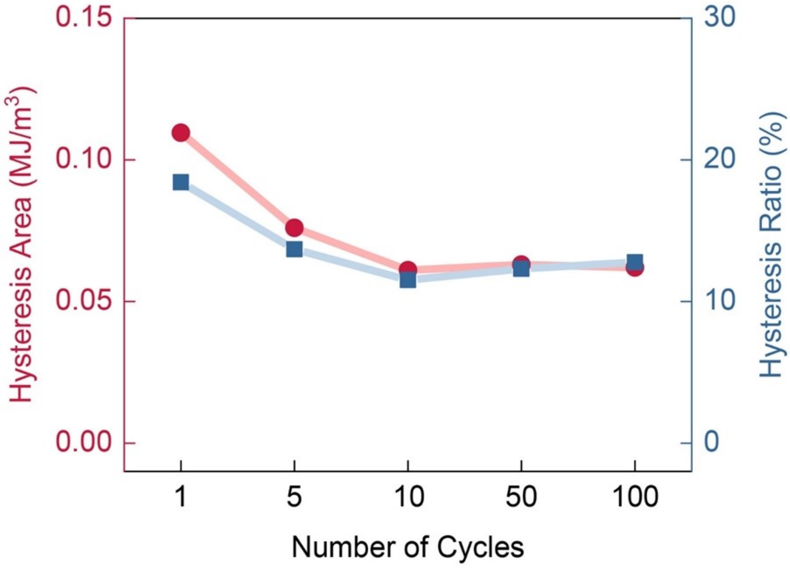

Fig. S7. Plot of hysteresis ratio versus the number of stretching-releasing cycles of Ionogel-4050-2% in the strain of 400% at a deformation rate of 100 mm min^{-1}.

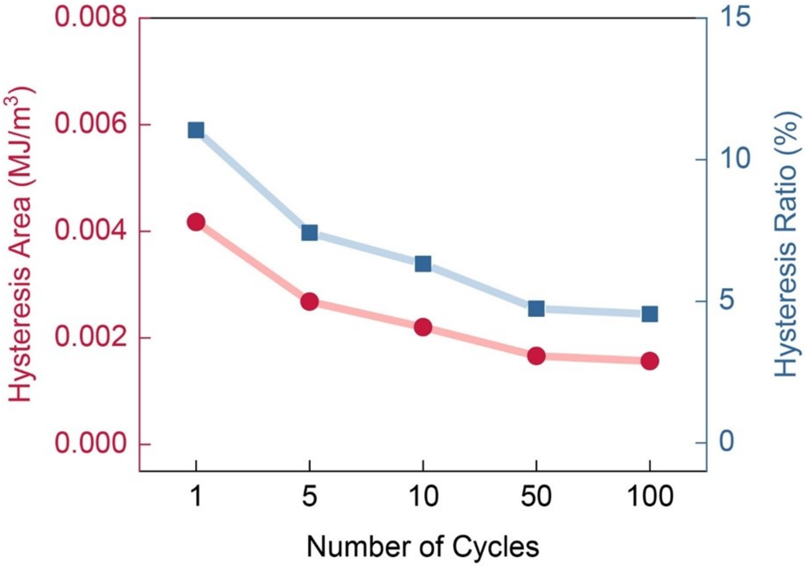

Fig. S8. Plot of hysteresis ratio versus the number of compressing loading-unloading cycles of Ionogel-4050-2% under a compression of 1 MPa.

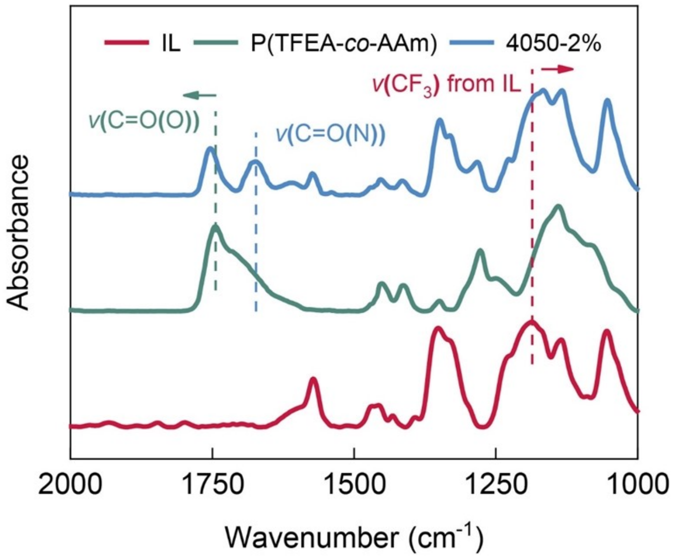

Fig. S9. FT-IR spectra and assignments of the ionic liquid (IL), P(TFEA-*co*-AAm), and Ionogel-4050-2%. The strong absorption peaks at 1186 cm^{-1} corresponding to the $\nu(CF_3)$ of the IL shifted slightly to 1166 cm^{-1} in the Ionogel-4050-2%, indicating the presence of ion-dipole interactions.

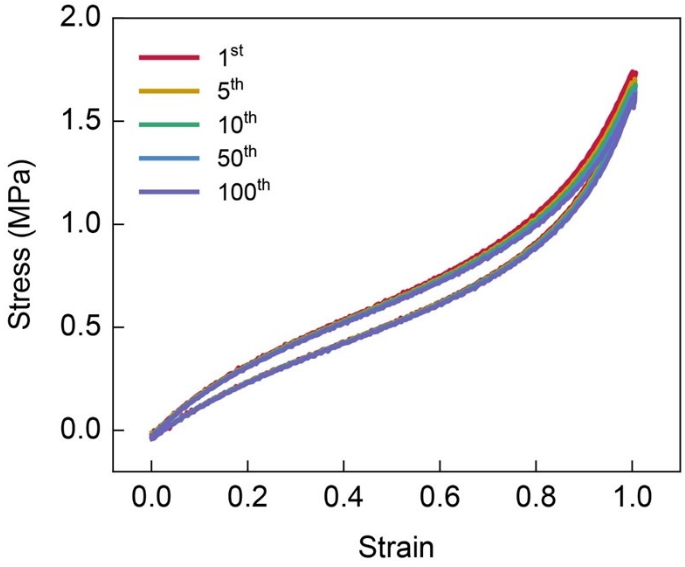

Fig. S10. Cyclic stretching-releasing curves of the PDMS dielectric thin film with a thickness of 100 μm at a fixed strain of 100% for 100 cycles without interval. The Nearly overlapping stretching-releasing curves reveals robust resilience.

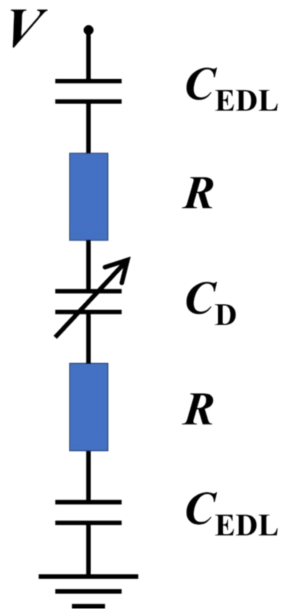

Fig. S11. Equivalent circuit of the iCPS consists of three capacitors and two resistors connected in series. Under deformation, the capacitance of the variable capacitor C_D, which represents the capacitor formed by the ionogel electrodes and a dielectric layer, is changed. This variation is monitored by the LCR and enables an accurate sensing of the pressure.

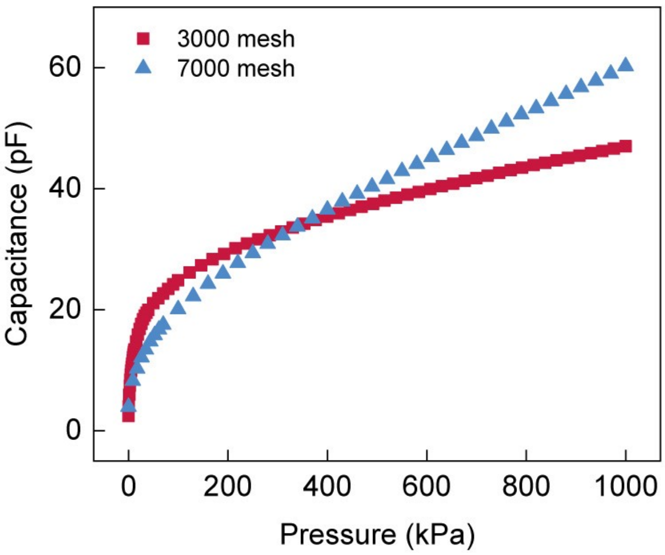

Fig. S12. Real capacitance-pressure response curves of the iCPS prepared by sandpapers with mesh sizes of 3000 and 7000, respectively.

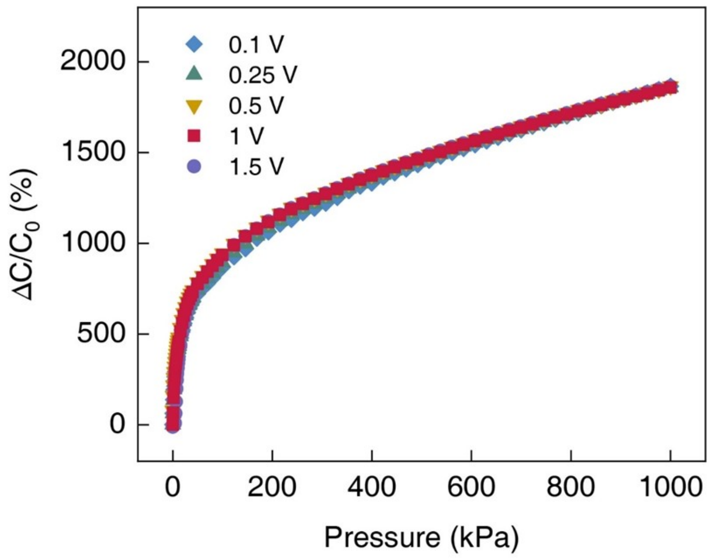

Fig. S13. Effect of varying the voltage platform on the sensing performance of the iCPS under a frequency of 1 kHz.

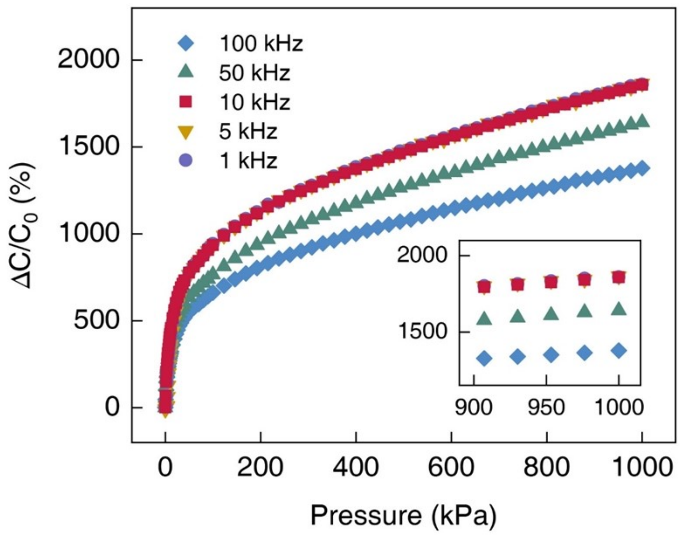

Fig. S14. Effect of varying the measurement frequency on the sensing performance of the iCPS under a voltage of 1V.

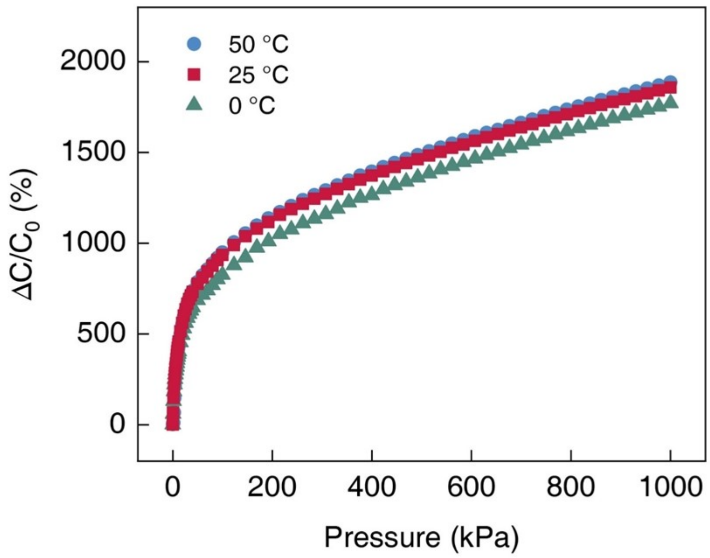

Fig. S15. Pressure-response behaviors of the iCPS under different temperatures.

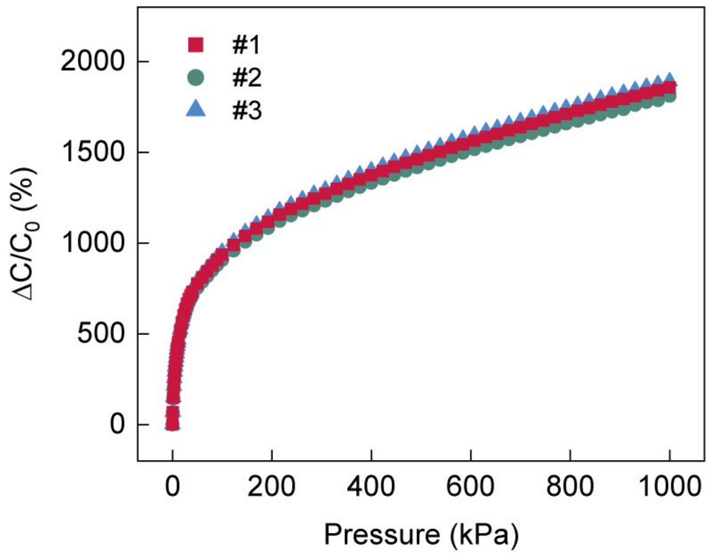

Fig. S16. Reproducibility test for capacitance change with the pressure of three iCPS devices made from different batches of sandpapers as the template.

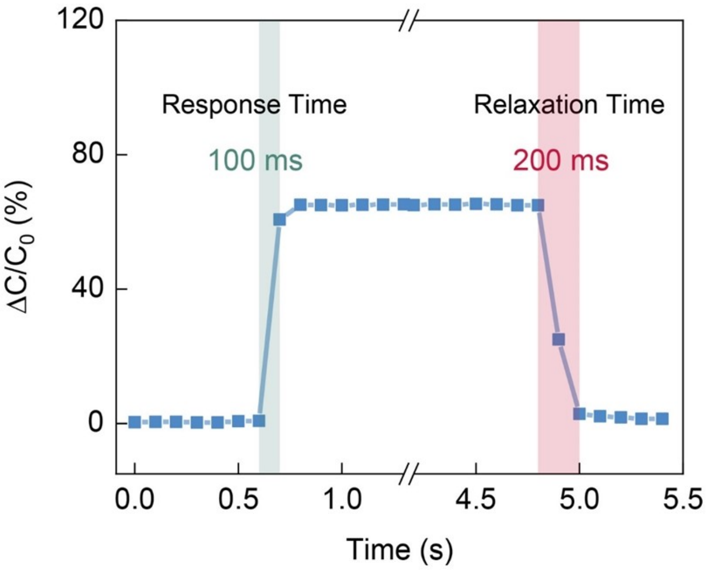

Fig. S17. Response and relaxation times of the iCPS were measured to be 100 and 200 ms, respectively.

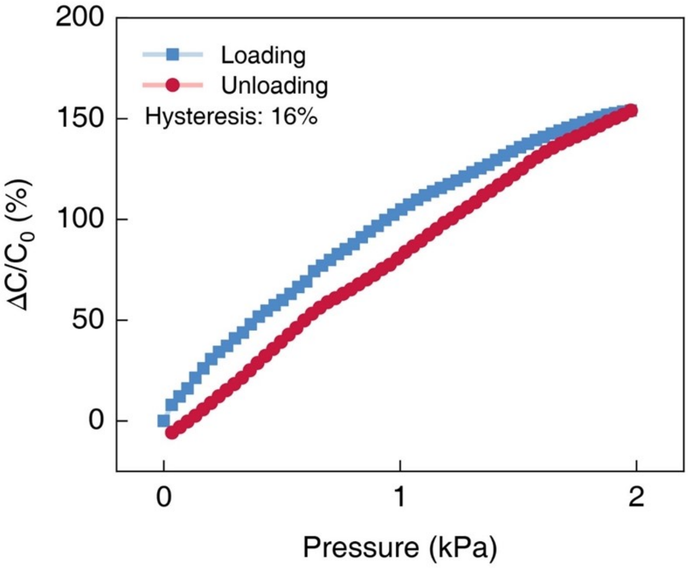

Fig. S18. Hysteresis of the iCPS under loading and unloading cycle.

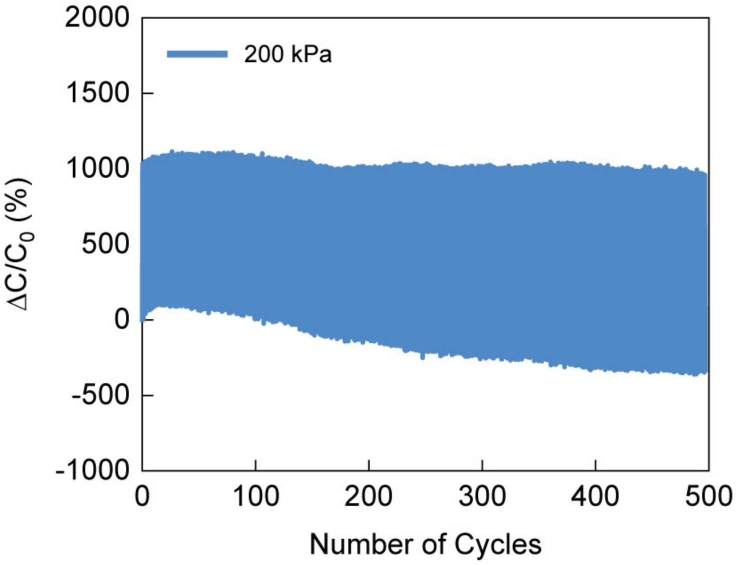

Fig. S19. Long term cyclic compressing-releasing test of the iCPS over 500 cycles under a pressure of 200 kPa.

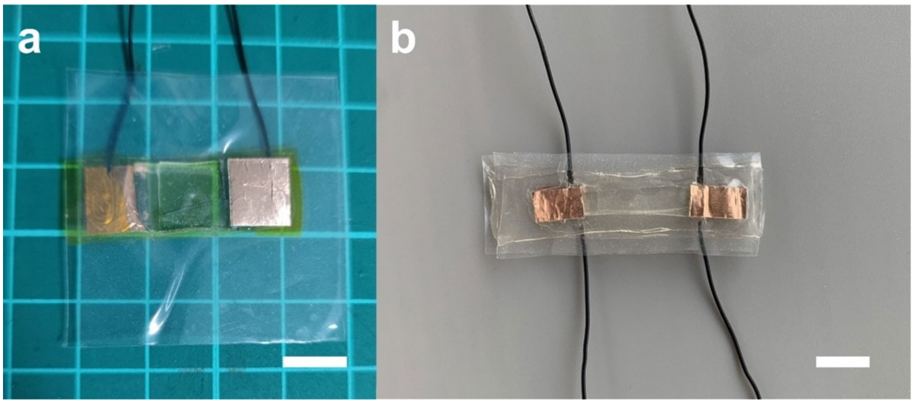

Fig. S20. Photographs of the iCPS with (a) a square configuration (10 mm × 10 mm, scale bar: 10 mm), and (b) a strip configuration (20 mm × 6 mm, scale bar: 10 mm).

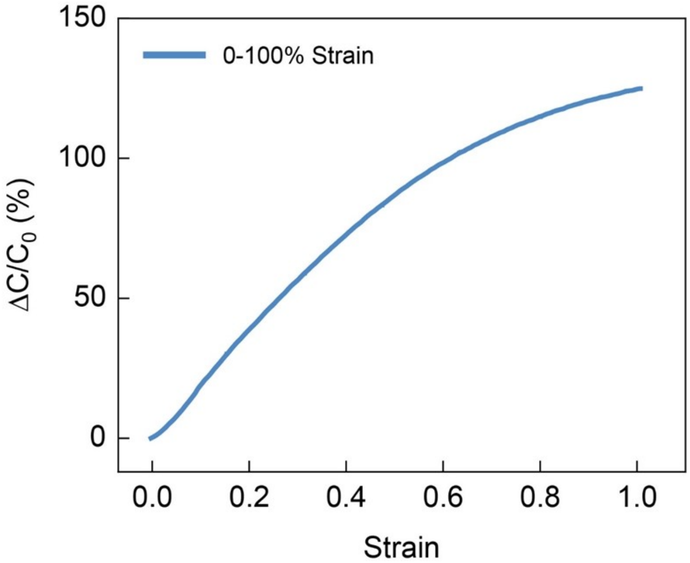

Fig. S21. Capacitance responses of the iCPS as a function of tensile strain range up to 100%.

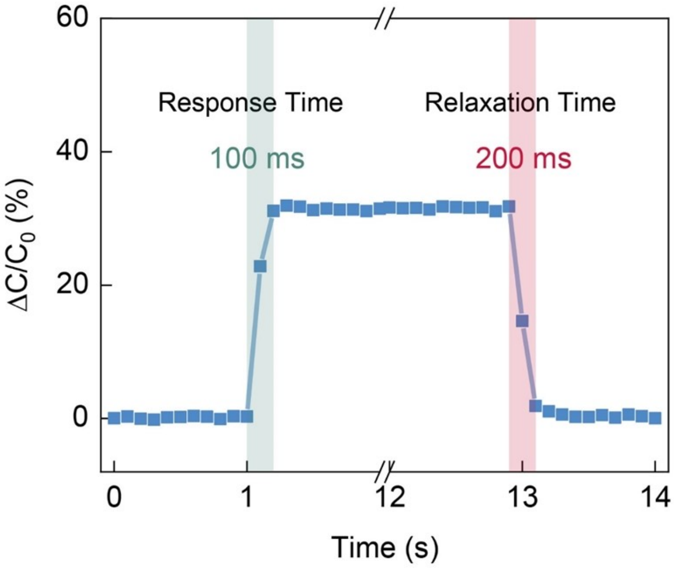

Fig. S22. Response and relaxation times of the iCPS under a 100% in-plane tensile deformation.

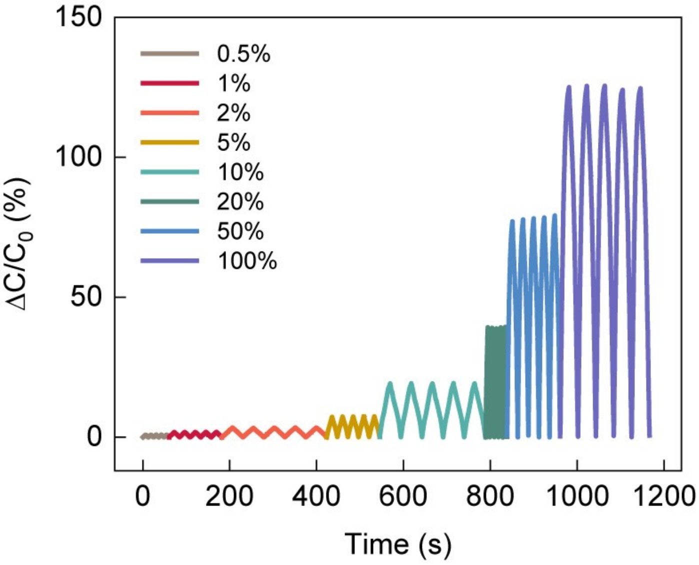

Fig. S23. Capacitance variations of the iCPS under successive tensile strain deformation range from 0.5% to 100%. The strain rates are set as 1, 5, and 50 mm/min in the strain ranges of 0.5-2%, 5-10%, and 50-100%, respectively.

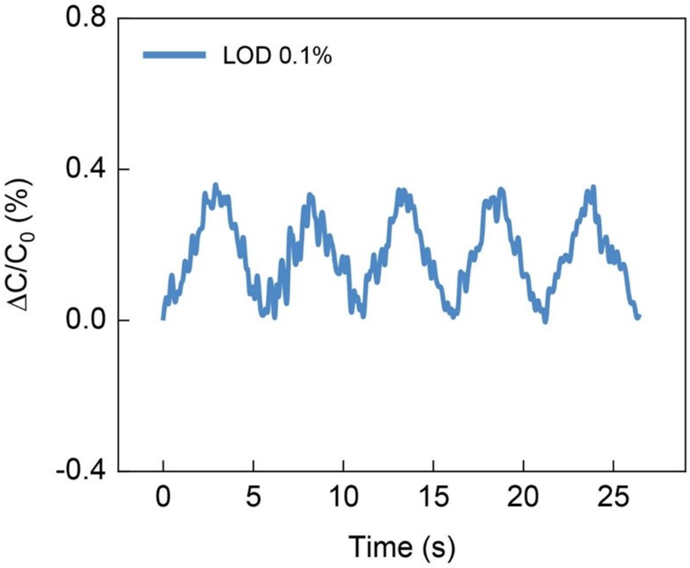

Fig. S24. The limit of detection (0.1%) of the iCPS for tensile strain deformation.

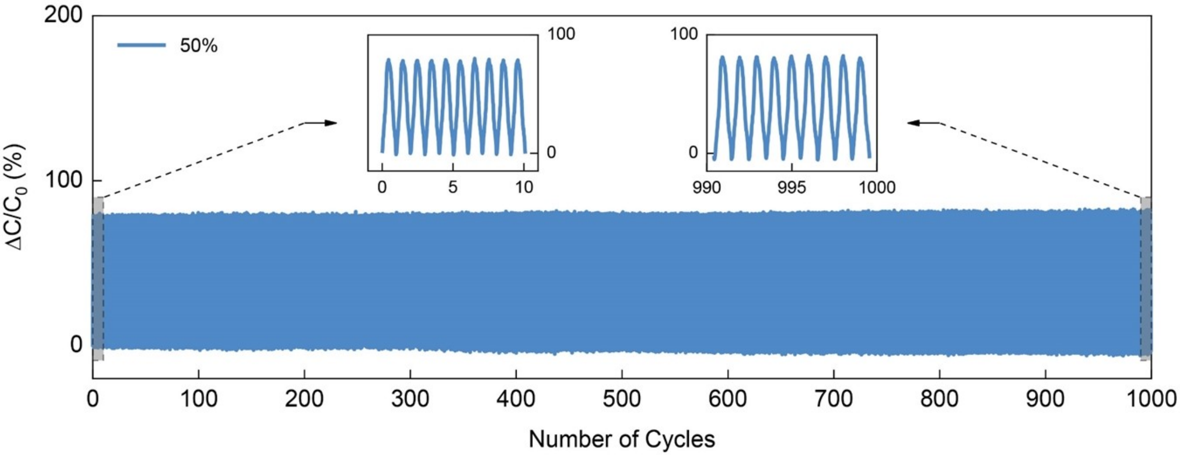

Fig. S25. Long term cyclic stretching-releasing test of the iCPS over 1000 cycles with cyclic strain from 0% to 50%.

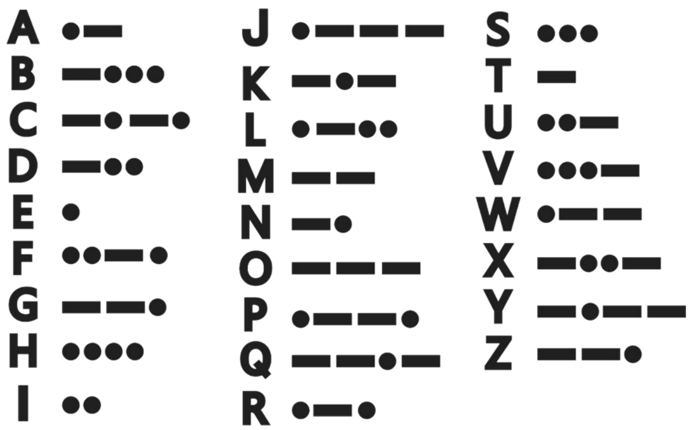

Fig. S26. Schematic diagram of Morse code.

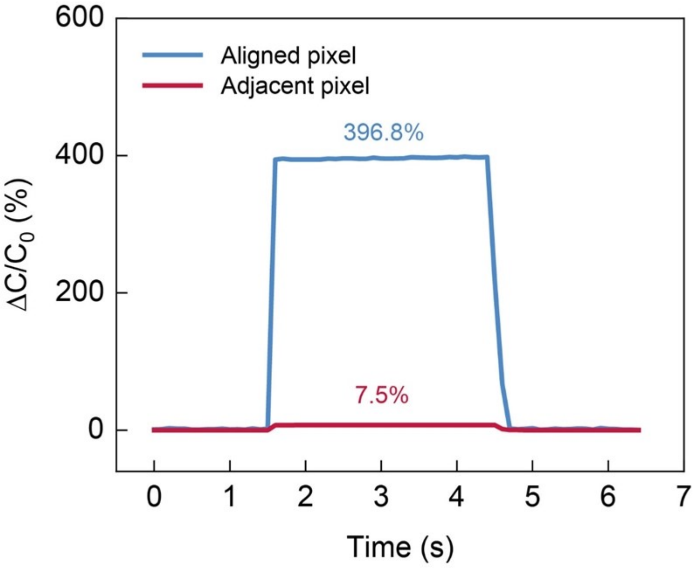

Fig. S27. Comparison of capacitance variations of a pixel with directly applied pressure versus an adjacent pixel in the sensor array. The pixel with alignment pressure exhibits 53 times larger capacitance than the adjacent pixel.

Table S1-S3.

Table S1. Summary of the formula for the preparation of the ionogels as the ionotronic electrodes.

Composite abbreviations	**Polymer mass fraction (%)**	**Monomer molar ratio of TFEA/AAm**	**EGDMA cross-linker molar content**
Ionogel-4050	40	100:50	0%
Ionogel-4050-0.5%	40	100:50	0.5%
Ionogel-4050-1%	40	100:50	1%
Ionogel-4050-2%	40	100:50	2%
Ionogel-4050-5%	40	100:50	5%

Table S2. Summary of mechanical properties of the ionogels with different compositions.

Composition	**Maximum tensile strength (MPa)**	**Strain at break (%)**	**Young`s modulus (kPa)**	**Toughness (MJ m^{-3})**
Ionogel-4050	0.55 ± 0.01	1828 ± 16	58 ± 9	3.66 ± 0.09
Ionogel-4050-0.5%	0.83 ± 0.01	1419 ± 12	49 ± 5	3.15 ± 0.06
Ionogel-4050-1%	0.53 ± 0.01	844 ± 47	60 ± 7	1.44 ± 0.11
Ionogel-4050-2%	0.52 ± 0.02	499 ± 33	89 ± 6	1.01 ± 0.14
Ionogel-4050-5%	0.50 ± 0.02	180 ± 18	215 ± 9	0.39 ± 0.18

Table S3. Comparison of our iCPS with previous representative works of stretchable pressure sensors.

	Capacitive				Resistive		
Ref.	**This work**	***Sci. Adv.* 7**, eabi4563 (2021).	***Nat. Electron.* 1**, 314 (2018).	***Nanoscale* 9**, 3834 (2017).	***Adv. Mater.* 26**, 3451 (2014).	***Adv. Mater.* 29**, 1703004 (2017).	***Nat. Mater.* 11**, 795 (2012).
Electrode	P(TFEA-*co*-AAm) [EMIM][TFSI] Ionogel	Ag paste/Ecoflex	Silver nanowire/ Polyester yarn	Mg/Polylactic acid	Conductive Fabric PEDOT:PSS/ Polyurethane	PEDOT:PSS/ SWCNT	Pt/PMDS
Dielectric layer	PDMS	PVDF/EMIM:TSFI/ HMDA ionic elastomer	PDMS/Dragon skin/Ecoflex	Poly(glycerol sebacate)	N/A	N/A	N/A
Sensitivity (kPa^{-1})	**0.802 (0-10 kPa) 0.034 (10-100 kPa) 0.010 (100-1000 kPa)**	4.5 (0-1 kPa) 2.0 (1-10 kPa)	0.012	0.13	2	0.005	0.13
Pressure sensing range (kPa)	**0-1000**	0-10	0-50	0-10	0-8	0-40	0-1.5
Max. working strain	**100%**	50%	40%	15%	40%	30%	4%
Limit of detection (Pa)	10	0.2	1.5	12	23	28	5
Strain-insensitivity	53%~75%	~98%	~0%	~0%	~63%	~65%	~30%
Response time of loading (ms)	100~200	50	31	c.a.150	200	c.a.62	50
Compression robustness (times)	8000	>500	10000	30000	N/A	N/A	N/A
Fabrication process	**Simple**	Complex	Complex	Complex	Complex	Complex	Complex

Movie S1-S6.

Movie S1. Finite element analysis of an electrode/dielectric/electrode interface in Plain-Plain configuration under pressures from 0 to 1 Mpa.

Movie S2. Finite element analysis of an electrode/dielectric/electrode interface in Rough-Plain configuration under pressures from 0 to 1 Mpa.

Movie S3. Finite element analysis of an electrode/dielectric/electrode interface in Rough-Rough configuration under pressures from 0 to 1 Mpa.

Movie S4. The accurate detection of finger touches by the iCPS.

Movie S5. The accurate detection of falling water droplets by the iCPS.

Movie S6. Demonstration of the stretchability and resilience of the iCPS at 100% tensile strain.